HAPTIC SUPPORT FOR AVOIDING STATIC AND DYNAMIC OBSTACLES IN UAV TELE-OPERATION

Tomasz Piessens, M. M. (René) van Paassen and Max Mulder
Aerospace Engineering – Delft University of Technology
Delft, The Netherlands

Impoverished sensory input makes tele-operation of Unmanned Autonomous Vehicles a difficult task. Automation support can provide assistance to the operator, but may also produce automation surprise and a risk of loss of situation awareness, when the human operator fails to notice the actions of automation in high-workload situations. Previous work applied haptic feedback based on an artificial risk field to assist in avoidance of static obstacles with a small helicopter UAV. An off-line analysis of that solution shows that it would not be sufficiently effective for the avoidance of dynamic, moving obstacles. A new haptic assist algorithm, based on velocity obstacle theory was developed. This algorithm was first tested in off-line analyses, in scenarios with only static obstacles and in scenarios with a dynamic obstacle added. The off-line analysis showed the feasibility of the algorithm. The algorithm was then ported to a real-time environment and evaluated in pilot-in-the loop simulations, to verify the solutions and investigate the acceptability of the haptic feedback. Results indicate that the velocity obstacle approach works for both stationary and moving obstacles, in most, but not all scenarios.

Remotely operating of a vehicle in most cases is associated with limitations in sensory input (Custers, Oerlemans, & Vergouw, 2015). Operating beyond the line-of-sight operators often rely on camera images only, with limited resolution and field of view (FOV), and lack the natural multi-sensory environment as compared to when they would be on-board the vehicle themselves. To assist these operators in flying a UAV in a cluttered, obstacle-laden environment, a haptic interface for collision avoidance has been developed (Lam, Mulder, & van Paassen, 2007; Ho, Borst, van Paassen, & Mulder, 2018). The system uses a sensor to detect objects in the surrounding, and from this calculates an artificial force field to determine the appropriate haptic force feedback for the control stick (Lam, Boschloo, Mulder, & van Paassen, 2009). This proved helpful in obstacle avoidance, however, the method by which this support system is tuned makes it appropriate to avoidance of *static* obstacles only. Similar approaches, also for static obstacles, have been reported in literature (Murphy, 2012). As far as known, no support system has been reported that incorporates avoidance for *dynamic*, moving obstacles.

With trends in UAV operations it will be likely that multiple UAVs will be operating in close vicinity, making collision avoidance support with moving obstacles all the more relevant. Through an off-line analysis, it was determined that the avoidance logic as used in (Lam et al., 2007) does not properly support the avoidance of a dynamic obstacle. To support safe operation, the obstacle avoidance support should therefore be extended, which is the aim of the current project. To this end, elements from similar approaches to (visual) display design in air traffic control and airborne collision avoidance (Van Dam, Mulder, & van Paassen, 2008; Ellerbroek, Brantegem, van Paassen, & Mulder, 2013; Ellerbroek, Brantegem, van Paassen, de Gelder, & Mulder, 2013; Mercado-Velasco, Borst, Ellerbroek, van Paassen, & Mulder, 2015) were used.

The obstacle avoidance support in (Lam et al., 2007) was limited to the horizontal plane only, and was based on a range sensor that provided distance to obstacles around the UAV, with a resolution of 500 lines covering the full 360 degrees around the vehicle. Since it cannot be assumed that the position of all moving obstacles is known through other surveillance means, a similar (LiDAR) sensor input is also used here. Whereas previous work in airborne conflict resolution and air traffic control support could use surveillance data to determine the location of moving obstacles, and assume a circular Protection Zone (PZ) around each obstacle, here the location of surrounding traffic is to be inferred from LiDAR sensor-like input data.

The paper is structured as follows. First, a very brief explanation of relevant Velocity Obstacle (VO) theory is given, followed by an overview of our Collision Avoidance System (CAS) design. A pilot-in-the-loop experiment and its results are discussed, followed by final conclusions and recommendations.

System Architecture

Velocity Obstacles

The Velocity Obstacle method, here applied only in the horizontal XY plane, calculates permissible vehicle velocities that will avoid dynamic or static obstacles in the environment.

To this end, the *relative* velocities between a moving obstacle and the controlled UAV that would end up in a collision, respectively a path too close to the obstacle, are determined, and mapped to the UAV's absolute velocity space (Mercado-Velasco et al., 2015).

This is illustrated in Figure 1. Here, the vehicle that is under control, vehicle B (with velocity V_B), is crossing paths with another vehicle, A (with velocity V_A). Knowing the velocities V_A and V_B and the minimum distance that the two vehicles should remain separated – a circular disk referred to as the Protected Zone (PZ' in Figure 1) – allows the calculation of all velocities and headings of vehicle B (as it is the vehicle considered under control, but it would work similarly when vehicle A would be considered) that would end up with vehicle B entering the PZ of vehicle A (Van Dam et al., 2008).

What results is the dented gray circle drawn around vehicle B, which shows all possible *and safe* speeds and headings for this vehicle. Possible, as it shows the minimum and maximum speed range as a circle, and safe because *some combinations of heading and speed result in a conflict with vehicle A.*

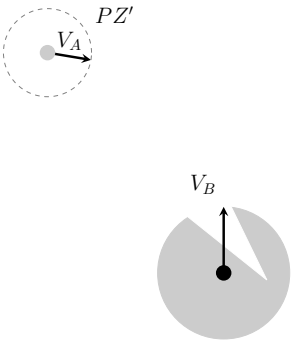

Figure 1: Bird's eye view of two moving vehicles in the horizontal XY plane.

Architecture

A scheme of the total system architecture for the Collision Avoidance System is given in Figure 2, it is composed of the following components:

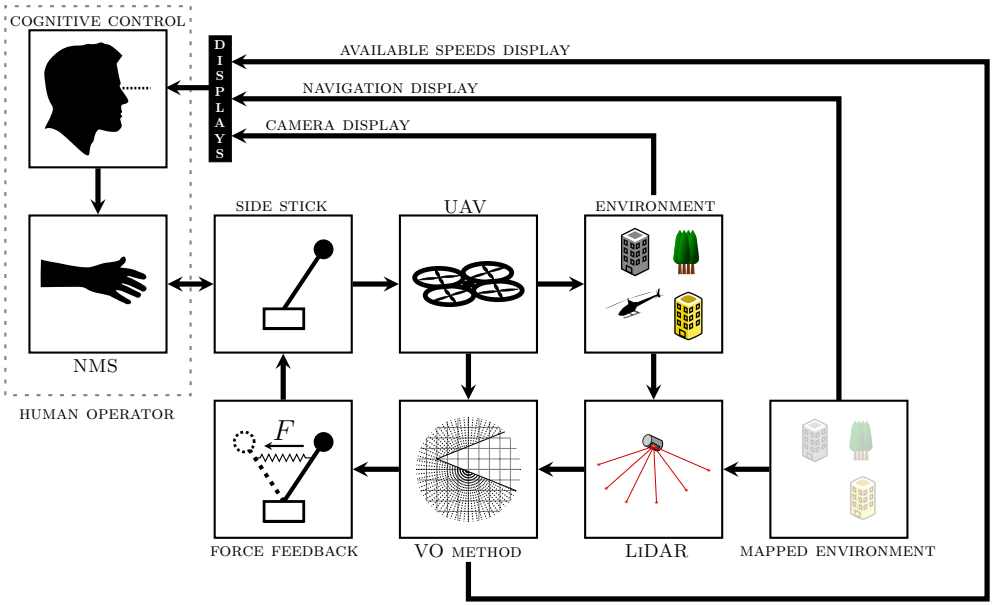

Figure 2: Schematic representation of the haptic Collision Avoidance System.

- The environment is sensed with a (simulated) LiDAR range finder, mapping dynamic and static objects onto a 2D plane, coded as range and bearing from the UAV. The environment is scanned with a resolution of 500 rays up to a distance of 100 $[m]$.

- Using a static map of the environment, measurements resulting from static obstacles are distinguished from the LiDAR range mapping. For static obstacles, the mapping as a velocity obstacle depends only on the vehicle's own velocity. A safety distance is added – as a circular buffer – onto the measurements. For this the super-positioning method for Protection Zones (PZ) from (Damas & Santos-Victor, 2009) is used.

- The static distances, with safety distance, are now translated into a maximum speed in the direction of the detected obstacle. A maximum acceleration/deceleration a_{max} of the controlled UAV in any given direction is assumed, then given a distance d_i to the obstacles in that direction, a modified form of the calculation given by (Damas & Santos-Victor, 2009) is used:

$$v_{max}(i) = \sqrt{f_s \cdot 2a_{max} \cdot d_i + (f_s \cdot a)^2_{max}\Delta T^2} - f_s \cdot a_{max} \cdot \Delta T \tag{1}$$

  Here ΔT is the discrete update time of the LiDAR system. The modification is the inclusion of a safety factor on the maximum possible acceleration, $f_s = 0.5$. This results in a permissible velocity map that accounts for static obstacles only.

- After the previous step, the measurements from the dynamics obstacles remain to be processed. It was originally attempted to determine the speed of dynamic obstacles from the measurements, as detailed for example in (MacLachlan, 2005), however, this proved to be impractical within the scope of the project. As a shortcut, the measurements were matched against a list of objects obtained from the simulation, producing the exact intruder velocity.

- The edges of the detected dynamic obstacles were determined, and using the detected distance, a cone of relative velocities that would bring the two vehicles too close together was determined. A radius of R_{total} is used there, composed of the radius of the own vehicle ($R_{UAV} = 1$ [m]) and a minimum safety distance $R_{pz} = 1.6$ [m], see Figure 3a.

- Using the respective intruders's velocities, the relative velocity cones are translated to the UAV's absolute velocity space, resulting in blocked zones in the permissible velocities, see Figure 3b.

- Given the current speed, the set of permissible speeds is searched for the closest permissible speed V_{safe}. The difference between the current speed and the closest safe speed is expressed as a speed magnitude change ΔV and a yaw angle change $\Delta\psi$, resulting in target normalized stick inputs for lateral and longitudinal control, respectively, x_{stick} and y_{stick}:

$$x_{stick} = \min\left(1, \max\left(\Delta\psi/0.32, -1\right)\right) \tag{2}$$

$$y_{stick} = \min\left(1, \max\left(\Delta V/4, -1\right)\right) \tag{3}$$

  This is rendered to a lateral and longitudinal haptic force with gains $K_{lat} = 2.5$ [Nm] and $K_{long} = 2.86$ [Nm] respectively.

Experimental Evaluation

A limited evaluation was performed with 5 participants, all right-handed, and none had previous experience in UAV tele-operation. The experiment was approved by the TU Delft Human Research Ethics Committee.

Apparatus and scenarios

The algorithm described above was programmed in the simulation used by (Lam, D'Amelio, Mulder, & van Paassen, 2006) in TU Delft's Human-Machine Interaction laboratory. A projected image was given of the front camera view of the controlled UAV, and head-down displays showed a map view based on the fixed obstacle database (Figure 4b) and a view of the available speeds calculation (Figure 4a). Figure 4c shows the set-up. The same vehicle simulation as used by (Lam et al., 2006) was used, and test tracks were generated from the same database.

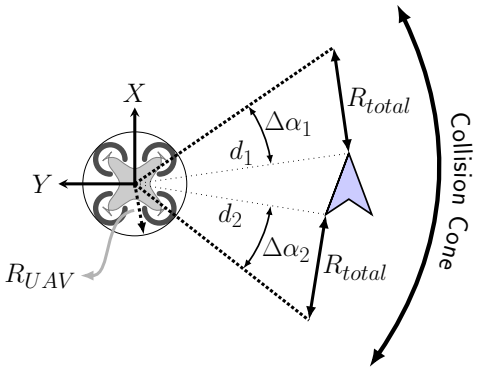

(a) The relative velocities blocked off by the intruder are constructed by adding a radius R_{total} to points detected at the edges of the obstacle.

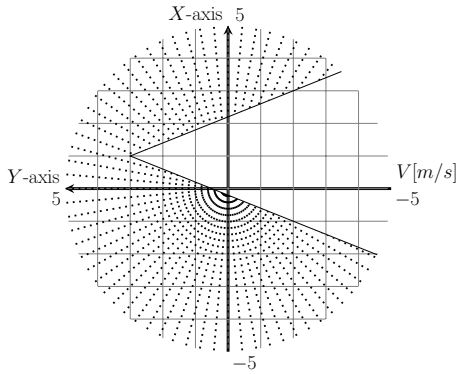

(b) After using the intruder's speed to translate the blocked relative velocities to the UAV's velocity space, a set of permissible velocities remains.

Figure 3: Calculation of permissible velocities in the presence of a moving obstacle.

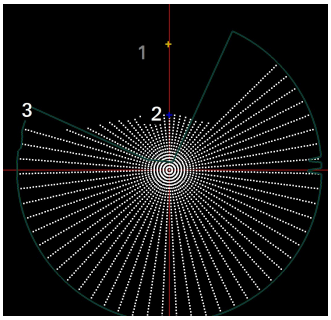

(a) Speeds display

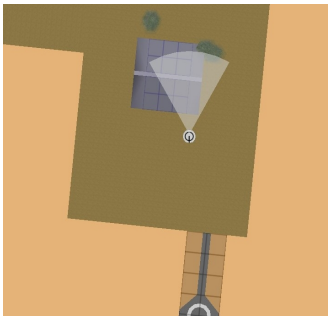

(b) Map view

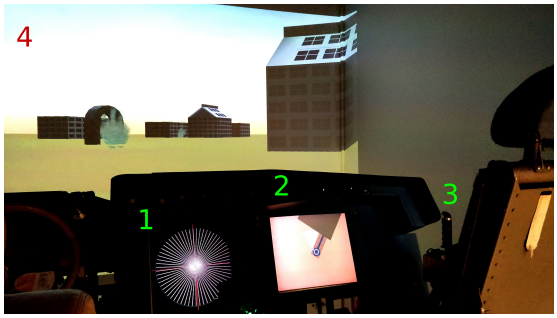

(c) Laboratory set-up

Figure 4: Experiment displays (left, middle) and laboratory set-up (right). In the right subfigure, '1' indicates the speeds display, '2' the map view, '3' the side stick, and '4' the outside view (simulated camera image).

Dynamic objects were added to the simulation and visualized as UAV's. These would appear and start moving when the operator controlled UAV would pass a trigger line in the database. Three simulated intruder traffic situation were used, illustrated in Figure 5:

Intruder 1 This obstacle appears around the corner when the operator is performing the maneuver of flying along a wall. The goal was to test the effectiveness of the CAS on obstacles that appear suddenly and become visible to the operator on the very last moment.

Intruder 2 This obstacle would cross paths with the UAV in the open field and would lead to a collision if the operator wouldn't adjust heading or speed. The obstacle was in the operators FOV the whole time.

Intruder 3 This obstacle would approach the UAV head on, while flying through a corridor. The operator would have ample time ($\pm\,15\,[s]$) to get out of the corridor before the obstacle would actually cause a collision. This scenario was chosen to check the behavior of the CAS when a conflict is created in a confined space.

Experiment design

Participants were instructed to fly the given course and avoid collisions with buildings or moving obstacles. The course was marked with waypoints that were represented by smoke plumes through which the operator had to navigate the UAV (Ho et al., 2018). In addition, participants were asked to fly through the waypoints as close as

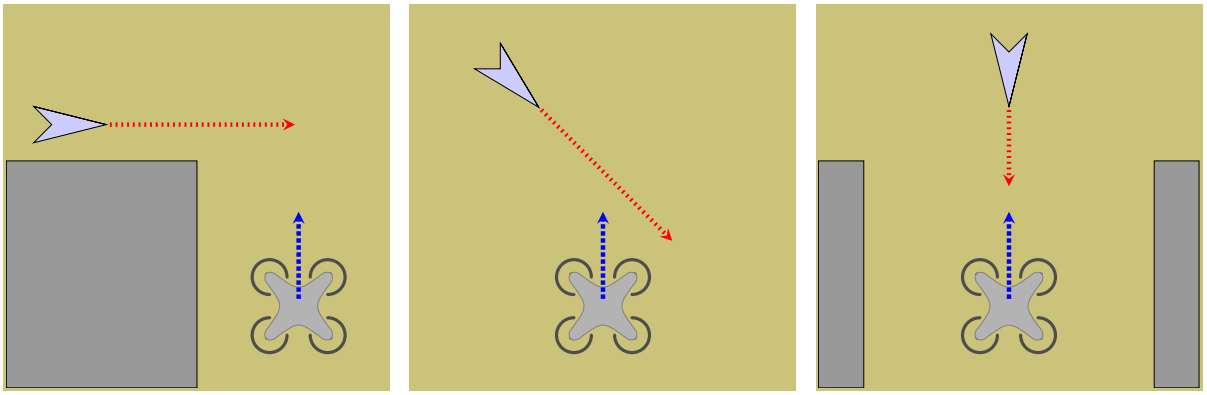

(a) Situation 1 *(b)* Situation 2 *(c)* Situation 3

Figure 5: The three flight situations with the intruder aircraft: (1) around the corner, (2) crossing in the open field, and (3) head-on in a corridor.

possible and to complete the course as fast as possible. If the UAV would have a collision, the screen would freeze for 5 seconds and the UAV would be placed back into the position just prior to the collision. Two training runs were performed prior to the start of the experiment. Each participant flew two measurement runs with each three sectors, with each sector having several static obstacles and one intruder aircraft. Runs with and without haptic feedback were balanced between subjects, the permissible speeds display was shown in all runs.

It was hypothesized that the haptic feedback would increase safety of the runs, to be verified from the number of collisions, that it would make the task easier, to be tested from a mental workload rating, but that the physical workload, to be determined from level of exerted force, might increase.

Results

Safety

Safety was measured by counting the number of collisions and measuring the minimum separation D_{min} between the UAV and the moving obstacles. Even with the small scale of the experiment, a nonparametric Friedman test indicated that the number of collisions differed significantly ($p < 0.05$). The collisions were further investigated, and it seems that all collisions due to the moving obstacle with the CAS active were with the third intruder scenario, in which the intruder was encountered in a small corridor, indicating that the CAS was not sufficiently supporting in that scenario.

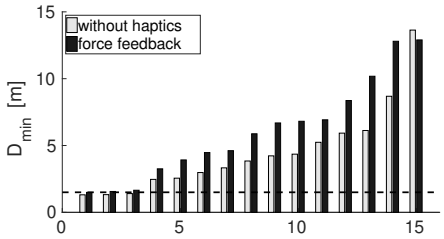

Figure 6: Minimum separation between UAV and intruder, sorted in size; not paired per intruder, for CAS active and inactive.

The minimum distance from intruder was investigated to determine the effect of the CAS on the flight, see Figure 6, which clearly shows that the CAS had a significant beneficial effect on avoidance of the intruder. Note that the figure shows the results of all fifteen runs (five subjects, three intruder scenarios).

Effort

The standard deviation of the exerted force in longitudinal direction and in lateral direction was determined and averaged for the runs with and without CAS. For the longitudinal input the stick force was increased by a considerable amount, 0.76 [Nm] versus 0.45 [Nm] without CAS. Workload was measured through the NASA TLX. No significant differences were found for the mental workload.

There was one "reverse parking" maneuver in each of the sectors of the scenario, and in the scenario with intruder #3 the UAV had to be reversed to avoid the intruder. These maneuvers in particular were associated with high stick forces, with the participants' input often conflicting with the input from the CAS, indicating that tuning and/or logic of the CAS were not appropriate for these situations.

Conclusions

The developed CAS supports operators in avoiding collisions with both static and dynamic obstacles, as apparent from the results of a limited evaluation. Operation in narrow spaces, particularly when travelling backwards, however, are not properly supported, and in these conditions the CAS tended to produce large and fluctuating lateral forces on the stick. No significant differences in workload were measured, however physical control forces and thus physical workload were higher.

Further optimization of the CAS, especially directed at maneuvers in narrow spaces, and investigation of scenarios where *both* UAV would be fitted with such a CAS, is warranted. Within the project there was no room to properly determine intruder velocity from the measured sensor values. Sources indicate that LiDAR sensors are able to perform this calculation, but these developments are not reported in open literature (MacLachlan, 2005).

References

Custers, B. H. M., Oerlemans, J. J., & Vergouw, S. J. (2015). *Het gebruik van drones*. Wetenschappelijk Onderzoek- en Documentatie Centrum (in Dutch).

Damas, B. & Santos-Victor, J. (2009). Avoiding moving obstacles: The forbidden velocity map. In *Proc. ieee/rsj int. conf. on intelligent robots and systems*.

Ellerbroek, J., Brantegem, K. C. R., van Paassen, M. M., de Gelder, N., & Mulder, M. (2013). Experimental evaluation of a coplanar airborne separation display. *IEEE Trans. on Human-Machine Systems*, *43*(3), 290–301.

Ellerbroek, J., Brantegem, K. C. R., van Paassen, M. M., & Mulder, M. (2013). Design of a coplanar airborne separation display. *IEEE Transactions on Human-Machine Systems*, *43*(3), 277–289.

Ho, V., Borst, C., van Paassen, M. M., & Mulder, M. (2018). Increasing acceptance of haptic feedback in UAV teleoperation by visualizing force fields. In *Proceedings of the IEEE international conference on systems, man, and cybernetics* (pp. 3023–3028). Myazaki (Japan).

Lam, T. M., Boschloo, H. W., Mulder, M., & van Paassen, M. M. (2009). Artificial force field for haptic feedback in UAV tele-operation. *IEEE Transactions of Systems, Man & Cybernetics, Part A*, *39*(6), 1316–1330.

Lam, T. M., D'Amelio, V., Mulder, M., & van Paassen, M. M. (2006). UAV tele-operation using haptics with a degraded visual interface. In *Proceedings of the IEEE conference on systems, man & cybernetics (IEEE-SMC)* (pp. 2440–2445). Taipei, Taiwan.

Lam, T. M., Mulder, M., & van Paassen, M. M. (2007). Collision avoidance in UAV tele-operation with time delay. In *IEEE international conference on systems, man and cybernetics* (pp. 997–1002). Montreal, Canada: IEEE.

MacLachlan, R. (2005). *Tracking moving objects from a moving vehicle using a laser scanner* (Technical Report No. CMU-RI-TR-05-07). Robotics Institute -Carnegie Mellon University. Pittsburg, PA.

Mercado-Velasco, G. A., Borst, C., Ellerbroek, J., van Paassen, M. M., & Mulder, M. (2015). The use of intent information in conflict detection and resolution models based on dynamic velocity obstacles. *IEEE Transactions on Intelligent Transportation Systems*, *16*(4), 2297–2302.

Murphy, R. R. (2012). A decade of rescue robots. *International Conference on Intelligent Robots and Systems,* 5448–5449.

Van Dam, S. B. J., Mulder, M., & van Paassen, M. M. (2008). Ecological interface design of a tactical airborne separation assistance tool. *IEEE Transactions on Systems, Man and Cybernetics, Part A*, *38*(6), 1221–1233.